Sensors and Materials, Vol. 35, No. 12 (2023) 4481–4489
MYU Tokyo

S & M 3492

Multicriteria Gear Monitoring System Based on Deep Neural Networks

Chia-Hung Lai[1*] and Ting-En Wu[2]

[1]Department of Intelligent Automation Engineering, National Chin-Yi University of Technology, No. 57, Sec. 2, Zhongshan Rd., Taiping Dist., Taichung 411030, Taiwan (R.O.C.)
[2]Department of Industrial Education and Technology, National Changhua University of Education, No. 2, Shi-Da Road, Changhua City 50074, Taiwan (R.O.C.)

(Received August 3, 2023; accepted December 8, 2023)

Keywords: gear wear, vibration, condition monitoring

Gears are commonly used mechanical components in various fields of power transmission. They offer stability and high transmission efficiency. However, the issue of gear lifespan remains unavoidable. In this study, we have developed a gear monitoring system that employs deep neural networks (DNNs) and integrates data from the time domain, frequency domain, short-time Fourier transform (STFT), and discrete wavelet transform (DWT). This system is designed to monitor the occurrence of wear in both spur and helical gears. In this research, we expand its practical applications, implement various gear fault detection methods based on deep neural networks, provide multicriteria for gear monitoring, and offer experimental results demonstrating its effectiveness.

1. Introduction

Gears are one of the frequently used mechanical components in the field of transmission. Gears provide stable transmission and high transmission efficiency. However, the issue of gear lifespan has become unavoidable. Damage to gears can affect transmission efficiency and even lead to mechanical damage. With the continuously increasing demands for gear precision, gear inspection requires a substantial amount of time. Therefore, a gear monitoring system is needed to assist in handling issues related to gear fault detection and other related concerns.

Fault detection in gear monitoring systems can primarily be categorized into two types: wear and tooth breakage. Feng *et al.*[(1)] used a model to simulate the vibration of gearbox gears, comparing differences with and without lubrication to effectively predict wear and surface pitting in spur gears. Chin *et al.*[(2)] compared lubricated and unlubricated conditions, as well as different speeds and loads, to better monitor gear wear and vibration by studying transmission errors. Antoni *et al.*[(3)] measured gears at fixed frequencies and intervals until complete failure, revealing that abnormal spectral peaks appear when the gear is on the verge of failure, and determined the best signal-to-noise ratio. Sharma and Parey[(4)] conducted fault detection in gears

*Corresponding author: e-mail: chlai@ncut.edu.tw
https://doi.org/10.18494/SAM4709

ISSN 0914-4935
https://myukk.org/

by acquiring vibration signals, testing under various loads at the same speed, and found that internally mounted accelerometers outperformed traditional external accelerometers in fault characterization. Kane and Andhare[5] classified gear faults using psychoacoustics, acoustics, and vibration features, and discovered that statistical features from vibration signals were more informative than those from acoustic signals. Praveenkumar *et al.*[6] diagnosed automotive gearbox conditions through a monitoring system and implemented time-domain and frequency-domain decision trees, demonstrating their efficiency in shortening detection time. Hu *et al.*[7] assessed the impact of wear on gear pairs through vibration parameters, suggesting that combining the proposed indicators with vibration analysis is effective for detecting gear wear and faults. Brethee *et al.*[8] observed the wear condition of helical gears through monitoring, changing gear parameters and loads, and noted that with increased wear, the effect on the meshing spectrum peaks of helical gears became more pronounced. Antoniadou *et al.*[9] monitored the state of gearboxes using time-domain and frequency-domain analysis methods with various gearbox loads, and found that damaged gears exhibited periodic impulse-like harmonic frequencies in the meshing process. Lin *et al.*[10] utilized the artificial fish swarm algorithm for the detection of faults in ball bearings, revealing that this approach effectively enhances the accuracy of classification. Wang *et al.*[11] investigated the nonlinear dynamics of high-speed gas bearing systems, employing finite difference and hybrid methods. The study found that this methodology reduces damage caused by irregular vibrations in the system.

We present an efficient detection method by developing a gear monitoring system using a deep neural network (DNN) deep learning model. The collected signals are transformed into the time, frequency, and wavelet domains. Through DNN deep learning, gear faults are detected. The following are the primary contributions of this research.

1. A novel system for detecting gear faults is introduced and its practical applications are expanded.
2. Monitoring systems for both spur and helical gears are proposed.
3. Gear fault detection is based on DNN, providing a multi-standard detection method.
4. A 98% recognition rate for gear fault identification is achieved.

2. System Architecture

2.1 Short-time Fourier transform (STFT)

STFT is commonly used in signal processing, especially for nonperiodic signals. Mohammed and Rantatalo[12] found that by observing the changes occurring in the signal over time, anomalies can be effectively detected. Nentwich and Reinhart[13] observed that by STFT, the detection of gear cracks is effective in identifying gear defects. In monitoring the health status of industrial robot gears, this method, employing STFT, was found to be comparable to using the RMS indicator. It involves dividing the time-domain signal into multiple short-time windows and performing a Fourier transform on each of these windows. The formula for STFT is

$$x(t,f)=\int_{-\infty}^{\infty}x(\tau)\omega(t-\tau)e^{-j2\pi f\tau}d\tau, \tag{1}$$

where $x(t, f)$ represents the result after applying STFT in both time and frequency domains. $x(\tau)$ stands for the input signal. $\omega(t - \tau)$ is the window function used to segment the signal. j represents the imaginary unit, where $j^2 = -1$. Through STFT, it is possible to effectively adjust the resolution of the Fourier transform in the time domain. The larger the short-time window, the higher the resolution in the frequency domain. This makes it easier to distinguish information that may not be clear in terms of amplitude and time. In continuous time, the signals captured by the system appear in a discrete state. Therefore, we use the discrete Fourier transform (DFT) for calculations, transforming the signal into discrete frequency harmonic components.

The complexity of DFT is $O(n^2)$, where n represents the signal length. As the signal length increases, the required time increases at a square rate. Therefore, DFT is not suitable for processing large-scale operations. To save time when performing a Fourier transform on each window, fast Fourier transform (FFT) is used. The complexity of FFT is $O(n\log_2 n)$, where n still represents the signal length. The rate of increase in $\log_2 n$ is lower than that in n^2, making FFT a more efficient algorithm. In the frequency domain, $x(k)$ denotes the k-th quantity, and in the time domain, $x(n)$ represents the n-th sample. j stands for the imaginary unit and N is the length of signal samples. The formula for FFT is

$$x(k)=\sum_{n=0}^{N-1}x(n)e^{\frac{-j2\pi xn}{N}},\ (0\le k\le N-1). \tag{2}$$

FFT can transform signals. As shown in Fig. 1(a), in the time domain, signals change over time. Time-domain signals exhibit different numerical values at different time points and are typically represented as waveforms. Analyzing signals in the time domain can be challenging. Therefore, Fourier transformation is used to convert signals into the frequency domain, as depicted in Fig. 1(b). Wang *et al.*[14] showed that in the frequency domain, signals are represented by different frequencies and amplitudes. By extracting fault features from gear frequency samples through filtering and utilizing machine learning, the above-mentioned methods demonstrate exceptional effectiveness.

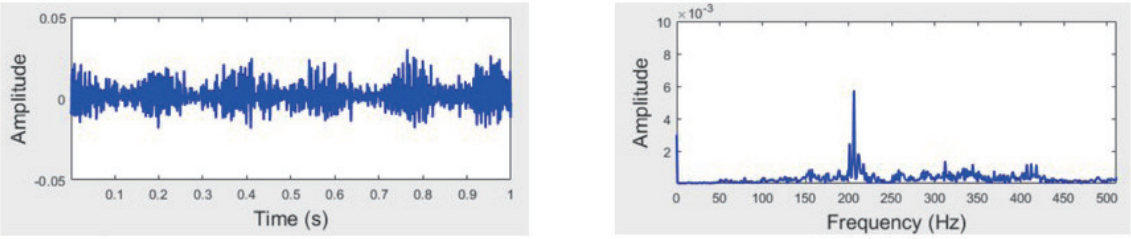

(a) (b)

Fig. 1. (Color online) (a) Time-domain signal. (b) Frequency-domain signal.

2.2 Discrete wavelet transform (DWT)

Discrete wavelet functions are effective in describing local features in signals and decomposing signals into different levels. During the decomposition process, both detail and low-frequency components are generated. Finally, these detail and low-frequency components are reconstructed.[15] Using DWT to extract fault features in gearbox, it was found that DWT filtering can diagnose gear faults early.[16] Classifying gearbox gears using the k-star algorithm and DWT results in very high accuracy.[17] Gear defects detected through DWT and EDM indicate that that combining support vector machine (SVM) with DWT yields excellent defect classification results. $DWT(j, k)$ represents discrete wavelet coefficients at level j and position k. $x(t)$ is the original discrete signal, with t denoting time. ψ stands for the wavelet function. The formula for DWT is

$$DWT\left(j,k\right)=\frac{1}{\sqrt{2^{j}}}\int_{-\infty}^{\infty}x\left(t\right)\psi\left(\frac{t-2^{j}k}{2^{j}}\right)dt. \tag{3}$$

2.3 DNN

DNN is a type of neural network model composed of input, hidden, and output layers. The input layer serves as the first layer of DNN and receives the initial input data. The hidden layer is the intermediate layer in a DNN model. It processes the data received by the first layer through weighted summation and activation, extracting features from the input data. The output layer is the final layer of the DNN model and is used to output classified data from the hidden layers.[18] The results of analyzing gear defect frequencies with DNN revealed that this method achieves a significantly high accuracy compared with convolutional neural network.[19] By applying variational mode decomposition (VMD) and DNN for planetary gear fault detection and using an autoencoder for gear state classification, this approach achieves an accuracy rate of 100%.[20] The results of DNN analysis of motor current signals for planetary gear fault diagnosis have demonstrated the superiority of DNN over other methods. The DNN architecture diagram used in this research is shown in Figure 2.

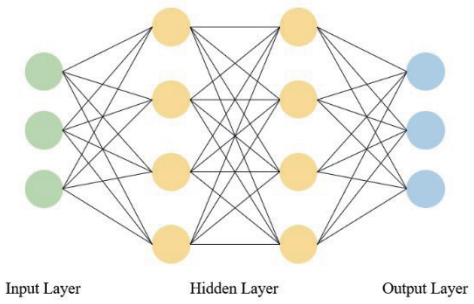

Fig. 2. (Color online) DNN architecture diagram.

3. Experimental Setup

We designed a gear defect detection model. Training was conducted using the DNN approach. Spur and helical gears of Module 3 were tested. Each gear consists of 30 teeth and the pinion has 20 teeth. The motor operates at 625 rpm. Accelerometers were placed on the bearings to record the gear-tooth vibrations while the motor runs. The recorded values were then transformed from the time domain to the frequency domain through STFT and DWT, and compiled into datasets. DNN models were trained separately on these datasets to determine the presence of gear wear. The detection equipment developed in this research consists of a gearbox (2) with a gear (12) and a pinion (11), and an accelerometer (3) on the bearing, as shown in Fig. 3.

The gear conditions set for this experiment simulated severe gear wear, as shown in Fig. 4. The sampling frequency for the vibration signal was 1024 Hz. A total of 819200 data points were collected over a sampling time of 800 s. The rotational speed was fixed at 625 rpm. For each condition, 800 sets of vibration signals were captured. The gear predominantly exhibited 50% wear, and this data was used for deep learning training. The training and testing data are presented in Table 1.

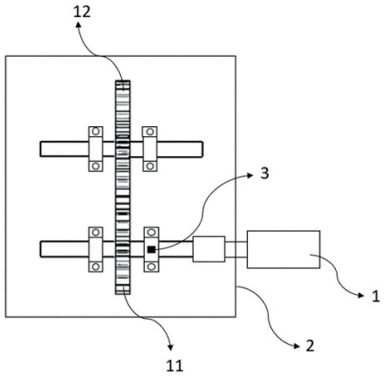

Fig. 3. Gear defect detection equipment.

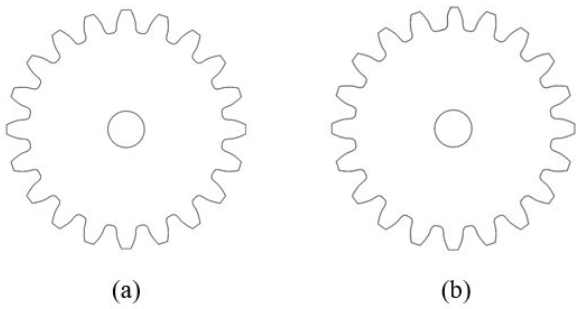

Fig. 4. (a) Healthy Gear. (b) Wear Gear.

Table 1
Training and testing data.

	Count
Training database	560
Verification database	160
Test database	80
Training database	640
Verification database	160
Test database	80

4. Results and Discussion

We use common spur and helical gears as detection targets. The collected time-domain signals are transformed into frequency-domain, STFT, and DWT signals. These signals are then processed using DNN to identify patterns associated with the healthy and worn states of gears.

In Fig. 5, it is observed that the amplitude of healthy spur gears falls within the range of −20 to −60. Among the 800 collected data points, the average amplitude is −54.1606. On the other hand, for worn spur gears, the amplitude varies between −20 and −80, with an average amplitude of −57.0262 among the 800 collected data points. Compared with healthy spur gears, worn spur gears exhibit more pronounced negative amplitudes. The change in the amplitude of the spur gear from −54 to −57 indicates the presence of wear in the gear.

In Fig. 6, it can be observed that the amplitude of healthy helical gears falls within the range of −20 to −80. Among the 800 collected data points, the average amplitude is −59.7765. For worn helical gears, the amplitude also ranges between −20 and −80, with an average amplitude of −62.9927 among the 800 collected data points. Compared with healthy helical gears, worn helical gears exhibit the most severe amplitudes between 0.5 and 1 s during the entire operation. The negative amplitudes of worn helical gears show a significant variation compared with healthy helical gears. The change in the amplitude of the helical gear from −59 to −62 indicates the presence of gear wear.

In Fig. 7, it can be observed that the average coefficient for healthy spur gears is ±0.029886914, whereas the average coefficient for worn spur gears is ±0.026037174. When the coefficient of the spur gear reaches approximately ±0.026, gear wear is considered to occur during operation. Therefore, it is recommended to replace the gear.

In Fig. 8, it can be observed that the average coefficient for healthy helical gears is ±0.020813182, whereas that for worn helical gears is ±0.014686684. When the coefficient of the helical gear reaches approximately ±0.0147, gear wear is considered to occur during operation. Therefore, it is recommended to replace the gear.

In Fig. 9, it can be observed that for spur gears, the time-domain, frequency-domain, STFT, and DWT data all exhibit very high accuracy. As for helical gears, the frequency-domain and STFT data show high accuracy. However, there is no significant difference observed in the time-domain signal and wavelet coefficient map for helical gears, suggesting that alternative methods are required for detecting faults in helical gears.

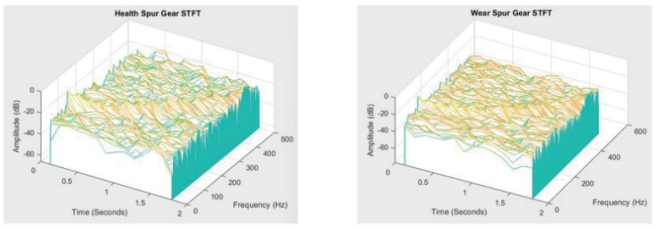

Fig. 5. (Color online) (a) Healthy spur gear waterfall chart. (b) Wear spur gear waterfall chart.

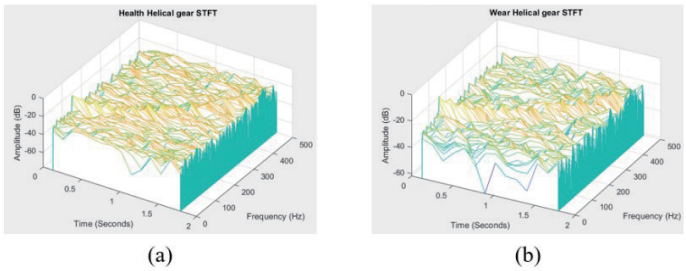

Fig. 6. (Color online) (a) Healthy helical gear waterfall chart. (b) Wear helical gear waterfall chart.

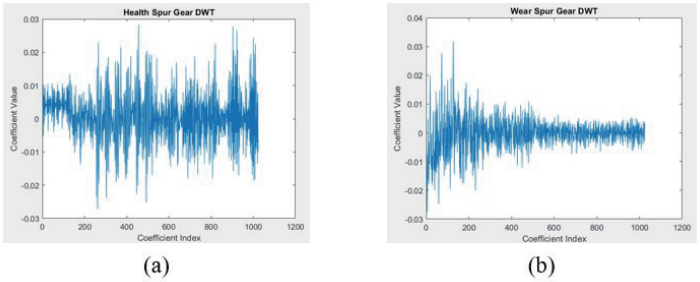

Fig. 7. (Color online) (a) Healthy spur gear coefficient chart. (b) Wear spur gear coefficient chart.

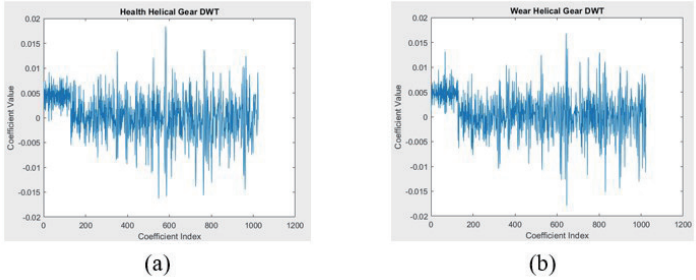

Fig. 8. (Color online) (a) Healthy helical gear coefficient chart. (b) Wear helical gear coefficient chart.

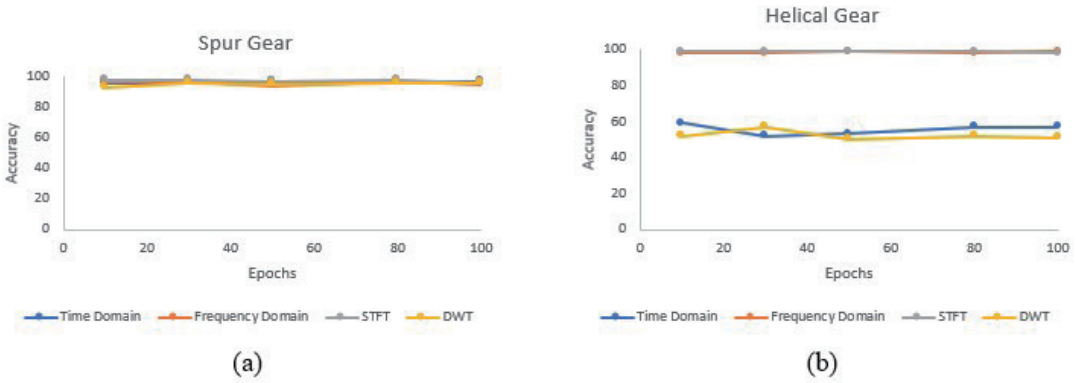

Fig. 9. (Color online) (a) Spur gear accuracy and epochs. (b) Helical gear accuracy and epochs.

5 Conclusions

In this study, we propose a gear wear detection system that utilizes data from the time domain, frequency domain, STFT, and DWT, which are then subjected to DNN deep learning. We also analyze the accuracy of gear monitoring through various methods to achieve the monitoring of both spur and helical gears. On the basis of the results of the comprehensive analysis of the obtained data, the following conclusions are drawn:

1. In this study, the collected data are subjected to FFT, followed by conversion into STFT and DWT representations. Finally, predictions are conducted in the time domain, frequency domain, as well as using STFT and DWT. Using the four different prediction results, we aim to identify the patterns associated with gear wear and provide a multicriteria detection approach.
2. Through the time-domain and DWT analyses, it was observed that the patterns of wear in spur gears are more easily identified than those in helical gears. Therefore, the time domain and DWT are well suited for use in the recognition of wear in spur gears.
3. Frequency-domain STFT analysis was found to exhibit very high accuracy in the recognition of wear in both spur and helical gears. Therefore, frequency-domain STFT is suitable for the recognition of wear in both spur and helical gears.
4. It can be observed from the training of DNN that the number of training iterations is not significantly correlated with the accuracy of the model.
5. In the future, further research in the field of gear monitoring can be pursued with a focus on expanding the dataset to include more cases of gear damage in order to provide a more comprehensive and robust gear monitoring system.

References

1 K. Feng, W. A. Smith, R. B. Randall, H. Wu, and Z. Peng: Mech. Syst. Signal Process. **165** (2022). 108319.
2 Z. Y. Chin, P. Borghesani, W. A. Smith, R. B. Randall, and Z. Peng: Wear **523** (2023) 204803.
3 J. Antoni and R. B. Randall: Mech. Syst. Signal Process. **20** (2006) 308.
4 V. Sharma and A. Parey: Recent Advances in Sustainable Technologies: Select Proc. ICAST **2020** (2021) 153–163.
5 P. V. Kane and A. B. Andhare: Measurement **154** (2020) 107495.
6 T. Praveenkumar, B. Sabhrish, M. Saimurugan, and K. I. Ramachandran: Measurement **114** (2018) 233.
7 C. Hu, W. A. Smith, R. B. Randall, and Z. Peng: Mech. Syst. Signal Process. **76** (2016) 319.
8 K. F. Brethee, D.Zhen, F. Gu, and A. D. Ball: Mech. Mach. Theory **117** (2017) 210.
9 I. Antoniadou, G. Manson, W. J. Staszewski, T. Barszcz, and K. Worden: Mech. Syst. Signal Process. **64** (2015) 188.
10 C. J. Lin, W. L. Chu, C. C. Wang, C. K. Chen, and I. T. Chen: J. Low Freq. Noise Vibr. Act. Control **39** (2020) 954.
11 C. C. Wang, R. M. Lee, H. T. Yau, and T. E. Lee: J. Low Freq. Noise Vibr. Act. Control **38** (2019) 1404.
12 O. D. Mohammed and M. Rantatalo: Mech. Syst. Signal Process. **66** (2016) 612.
13 C. Nentwich and G. Reinhart: Robotics **10** (2021) 80.
14 J. Wang, S. Li, Y. Xin, and Z. An: J. Vib. Eng. Technol. **7** (2019) 159.
15 R. Bajric, N. Zuber, G. A. Skrimpas, and N. Mijatovic: Shock and Vibration **2016** (2016) 1.
16 K. N. Ravikumar, C. K. Madhusudana, H. Kumar, and K. V. Gangadharan: Eng. Sci. Technol. Int. J. **30** (2022) 101048.
17 I. M. Jamadar, R. Nithin, S. Nagashree, V. P. Prasad, M. Preetham, P. K. Samal, and S. Singh: J. Fail. Anal. Prev. **23** (2023) 1.
18 J. Kim, J. Kim, and H. Kim: Machines **10** (2022) 659.
19 Y. Li, G. Cheng, C. Liu, and X. Chen: Measurement **130** (2018) 94.
20 F. Li, X. Pang, and Z. Yang: Measurement **145** (2019) 45.

About the Authors

Chia-Hung Lai currently serves as an assistant professor in the Department of Intelligent Automation Engineering at National Chin-Yi University of Technology. He received his B.S. and M.S. degrees from National Changhua University of Education, Taiwan, in 2009 and 2011 and his Ph.D. degree from National Cheng Kung University, Taiwan, in 2020. His research interests are in gear design and monitoring, cyber physics, and sensors. (chlai@ncut.edu.tw)

Ting En Wu is currently studying for a bachelor's degree at National Changhua University of Education Department of Industrial Education and Technology. His research direction lies in gear design, image recognition, and vibration analysis. (s1031127@gm.ncue.edu.tw)